MANTLE CONVECTION AND MAGMA PRODUCTION ON MARS: THE EFFECT OF A DENSE LAYER AT THE BASE OF THE MANTLE. Qingsong Li and Walter S. Kiefer, Lunar and Planetary Institute, 3600 Bay Area Blvd., Houston TX 77058 (li@lpi.usra.edu).

Introduction: Mars has remained volcanically active into the geologically recent past, as demonstrated both by low impact crater densities on some lava flows [1, 2] and by the radiometric ages of the shergottites, which are igneous meteorites from Mars [3, 4]. Mantle plumes are a good explanation for recent volcanism on Mars [5]. Prior plume models included many important effects: spherical axisymmetric geometry, partitioning of radioactivity between crust and mantle, realistic temperature-dependent rheology, a Mars-specific solidus, and the effects of water on the solidus and rheology [5-7]. These studies have assumed a single convective layer. If Mars went through a magma ocean phase, the resulting silicate differentiation and mantle overturn might have resulted in a chemically stratified mantle [8]. The possible effects of such stratification on the early volcanic and magnetic dynamo histories of Mars were explored by Elkins-Tanton et al. [9, 10]. Zaranek and Manga [11] explored how layered mantle convection affects martian thermal evolution using one-dimensional parameterized convection calculations. Here, we explore the effects of mantle layering on present-day heat flux and magma production using a spherical axisymmetric plume model.

Computational Approach: We use the spherical axi-symmetric version of CitCOM [12, 13] to simulate mantle convection on Mars. A particle ratio method [14] is used in the code to model thermochemical convection. The non-dimensional model domain (θ = 0-π/4, R = 1-2) is meshed with a 128×128 grid that has a typical mesh resolution of 13 km. Each element is assigned with 16 particles to trace chemical composition. The upper and lower boundaries are constant in temperature. The side boundaries are thermally insulated. All four boundaries are free-slip. The mantle viscosity is temperature dependent, obeying the Arrhenius viscosity law [15]. The activation energy is 160 kJ/mole [5]. Half of the radioactive elements [16] are differentiated into the crust. The buoyancy number, B, is the ratio between the chemical density difference between the layers and the thermal buoyancy [17]. We assume B=1, corresponding to a density difference of about 200 kg m^{-3} between the two layers. The actual density difference could be larger [8], but further increase in B does not modify the fluid dynamics [17]. The dimensional model parameters are the same as in [5]. An initial thermal perturbation is applied to generate a plume at the center of the model. The model has been run to reach a statistically steady-state for each model case.

We use Katz's melt fraction calculation formula, in which melt fraction is a function of solidus, liquidus and the mantle temperature [18]. The Katz's dry solidus model coincides well with the experimental results of martian analog composition [19]. Magma production is calculated using the formalism of Kiefer [6].

Results: In the case of complete differentiation of a 2000 km thick magma ocean, the resulting high-density lower mantle layer may be as much as 250 km thick. However, models with no magma ocean or only a partial magma ocean have also been proposed [20, 21], so we consider a range of bottom layer thickness (25-200 km). For relatively thin lower layers, the flow in the bottom layer is driven by shear coupling to the convective flow in the upper layer. The bottom layer may convect separately if it is sufficiently thick. We also consider a range of convective vigor (thermal Rayleigh number defined using the bottom viscosity varies from 5.7×10^6 to 3.3×10^7) and core-mantle boundary temperatures. An example thermal field is shown in Figure 1. Model parameters for this example case are: thickness of the chemical layer is 106 km; the thermal Ra defined at bottom viscosity is 1.0×10^7; activation energy is 160 kJ/mole; half of the radioactivity is in the crust; temperature difference across the mantle is 1900 °C.

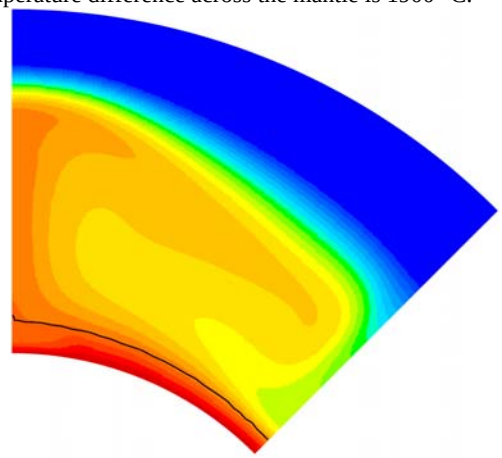

Figure 1. The super-adiabatic non-dimensional temperature is shown for the example case (see text). Color scale is 0.5 – 1.0 (blue to red). Temperature less than 0.5 is shown as blue. The black curve is the upper boundary of the dense layer.

Layer stability and interface topography. Previous simulations of convection in the mobile lid regime show that for a buoyancy number of 1, the deep dense layer is stable for geologically long periods of time but the interface between the two mantle layers may have significant topographic relief [17]. In contrast, our simulations for the stagnant lid regime show that for B=1, the deep layer is both stable for long times and that there is very little topographic relief on the interface between the two layers. This

is because in the stagnant lid regime, most of the thermal buoyancy is trapped in the stagnant upper boundary layer and is therefore not available to drive deformation of the deep layer. On Earth, interface topography in the D" layer may help to localize plumes [22], but our results suggest that this mechanism may not operate on Mars.

Effects on core heat flux. The core heat flux is suppressed by the inefficient heat transfer through the dense layer (Figure 2) that is consistent with previous predictions [17]. The decrease of core heat flux may be controlled by two mechanisms. First, when the dense layer is thin, its heat transfer is mainly through conduction. Increasing the layer thickness decreases the core heat flux. Second, when the layer is thick, it starts to convect, allowing more efficient heat transport through the dense layer. Thus, the core heat flux changes little as the layer thickness increases further.

The absence of a present-day magnetic dynamo places an upper bound on the heat flux out of the core of Mars [23]. Models with realistic rheology can produce plume volcanism while staying below this upper bound [5], but a chemically dense lower mantle layer may also contribute to suppressing the core heat flux and the magnetic dynamo.

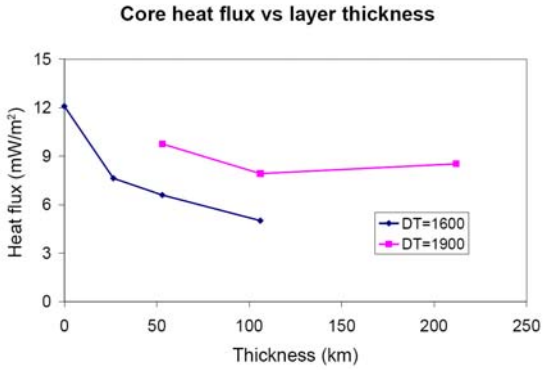

Figure 2. Core heat flux vs dense layer thickness for models with temperature differences of 1600°C (blue line) and 1900°C (red line) between the top and bottom of the mantle.

Effects on Magma production. In the example case, the non-dimensional temperature drop across the dense layer is ~0.1 (Figure 1), which is larger than the temperature drop across a purely thermal boundary layer [5]. The larger temperature drop across the dense layer causes a cooler mantle interior and a cooler plume. The core heat flux is also suppressed by the dense layer. Since the internal heating is constant, lower core heat flux causes lower surface heat flux, which indicates a thicker lithosphere. According to Li and Kiefer [5], both cooler plume and thicker lithosphere make it harder for decompression melting at the plume head. Besides the above effects, significant shear coupling may exist between the dense layer and overlying mantle. The shear coupling drags the chemical layer moving downward underneath the plume. The downwelling causes an inward heat flux below the plume (Figure 3), and may decrease the plume temperature relative to an unlayered mantle (Figure 1). However, the shear coupling may not be significant if the dense layer is vigorously convecting.

Future work. Our study of chemically stratified mantle convection on Mars is on-going and will extend our parameter space to include both thicker bottom layers and larger values of Ra. In addition, we intend to explore the effects of different material properties in the two layers, such as viscosity and thermal diffusivity [17] and partitioning of radioactivity between the two layers.

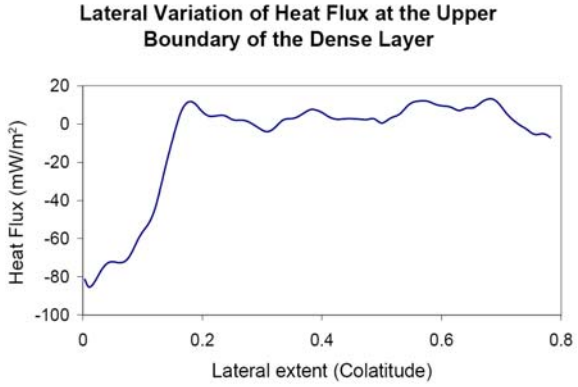

Figure 3. The lateral variation of heat flux at the upper boundary of the dense layer. The model parameters are the same as the case in figure 1. Negative values of heat flux correspond to heat flowing downward into the dense layer.

References: [1] Neukum et al., Nature 432, 971-979, 2004. [2] McEwen et al., Icarus 176, 351-381, 2005. [3] Nyquist et al., Space Sci. Rev. 96, 105-164, 2001. [4] Borg et al., Geochim. Cosmochim. Acta 69, 5819-5830, 2005. [5] Li and Kiefer, Geophys. Res. Lett. 34, doi:10.1029/2007GL030544, 2007. [6] Kiefer, Meteoritics Planet. Sci. 38, 1815-1832, 2003. [7] Li and Kiefer, Workshop on Water in Planetary Basalts, Abstract 2011, 2007. [8] Elkins-Tanton et al., Meteoritics Planet. Sci. 38, 1753-1771, 2003. [9] Elkins-Tanton et al., J. Geophys. Res. 110, doi:10.1029/2005JE002480, 2005. [10] Elkins-Tanton et al., Earth Planet. Sci. Lett. 236, 1-12, 2005. [11] Zaranek and Manga, Lunar Planet. Sci. Conf. 38, Abstract 2133, 2007. [12] Roberts and Zhong, J. Geophys. Res. 109, doi:10.1029/2003JE002226, 2004. [13] Zhong, J. Geophys. Res. 111, doi:10.1029/2005JB003972, 2006. [14] Tackley and King, Geochem. Geophys. Geosyst. 4, 8302, doi:10.1029/2001GC000214, 2003. [15] Mei and Kohlstedt, J. Geophys. Res. 105, 21471-21481, 2000. [16] Wänke and Dreibus, Phil. Trans. R. Soc. London A 349, 285-293, 1994. [17] Montague and Kellogg, J. Geophys. Res. 105, 11101-11114, 2000. [18] Katz et al., Geochem. Geophys. Geosyst. 4, 1073, doi:10.1029/2002GC000433, 2003. [19] Kiefer et al., Workshop on Water in Planetary Basalts, Abstract 2016, 2007. [20] Senshu et al., J. Geophys. Res. 107, 5118, doi:10.1029/2001JE001819, 2002. [21] Righter, Workshop on Early Planetary Differentiation, Abstract 4041, 2006. [22] Jellinek and Manga, Rev. Geophys. 42, doi:10.1029/2003RG000144, 2004. [23] Nimmo and Stevenson, J. Geophys. Res. 105, 11969-11979, 2000.